

Accepted Manuscript

Title: The selective reduction of NO_x with propene on Pt-beta catalyst: a transient study

Authors: J.M. García Cortés, M.J. Illán Gómez, C. Salinas Martínez de Lecea



PII: S0926-3373(07)00080-X
DOI: doi:10.1016/j.apcatb.2007.03.004
Reference: APCATB 9936

To appear in: *Applied Catalysis B: Environmental*

Received date: 13-11-2006
Revised date: 8-3-2007
Accepted date: 14-3-2007

Please cite this article as: J.M. García Cortés, M.J. Illán Gómez, C. Salinas Martínez de Lecea, The selective reduction of NO_x with propene on Pt-beta catalyst: a transient study, *Applied Catalysis B, Environmental* (2007), doi:10.1016/j.apcatb.2007.03.004

This is a PDF file of an unedited manuscript that has been accepted for publication. As a service to our customers we are providing this early version of the manuscript. The manuscript will undergo copyediting, typesetting, and review of the resulting proof before it is published in its final form. Please note that during the production process errors may be discovered which could affect the content, and all legal disclaimers that apply to the journal pertain.

**The selective reduction of NO_x with propene on Pt-beta
catalyst: a transient study**

J. M. García Cortés, M.J. Illán Gómez and C. Salinas Martínez de Lecea*

*Department of Inorganic Chemistry, University of Alicante, P.O. Box 99, E-03080
Alicante, Spain*

* Corresponding author.

Phone: +34 96 5903976

Fax: +34 96 5903454

E-mail: c.salinas@ua.es

Abstract

The mechanism of the NO/C₃H₆/O₂ reaction has been studied on a Pt-beta catalyst using transient analysis techniques. This work has been designed to provide answers to the volcano-type activity behaviour of the catalytic system, for that reason, steady state transient switch (C₃H₆/NO/O₂ → C₃H₆/Ar/O₂, C₃H₆/Ar/O₂ → C₃H₆/NO/O₂; C₃H₆/NO/O₂ → Ar/NO/O₂, Ar/NO/O₂ → C₃H₆/NO/O₂; C₃H₆/NO/O₂ → C₃H₆/NO/Ar and C₃H₆/NO/Ar → C₃H₆/NO/O₂) and Thermal Programmed Desorption (TPD) experiments were conducted below and above the temperature of the maximum activity (T_{max}). Below T_{max}, at 200°C, a high proportion of adsorbed hydrocarbon exists on the catalyst surface. There exists a direct competition between NO and O₂ for Pt free sites which is very much in favour of NO, and therefore NO reduction selectively takes place over hydrocarbon combustion. NO and C₃H₆ are involved in the generation of partially oxidised hydrocarbon species. O₂ is essential for the oxidation of these intermediates closing the catalytic cycle. NO₂ is not observed in the gas phase. Above T_{max}, at 230°C, C₃H_{6ads} coverage is negligible and the surface is mainly covered by O_{ads} produced by the dissociative adsorption of O₂. NO₂ is observed in gas phase and carbon deposits are formed at the catalyst surface. From these results, the state of Pt-beta catalyst at T_{max} is inferred. The reaction proceeds through the formation of partially oxidised active intermediates (C_xH_yO_zN_w) from C₃H_{6ads} and NO_{ads}. The combustion of the intermediates with O₂(g) frees the Pt active sites so the reaction can continue. Temperature has a positive effect on the surface reaction producing active intermediates. On the contrary, formation of NO_{ads} and C₃H_{6ads} are not favoured by an increase in temperature. Temperature has also a positive effect on the dissociation of O₂ to form O_{ads}, consequently, the formation of NO₂ is favoured by temperature through the oxygen dissociation. NO₂ is very reactive and produces the propene combustion without NO reduction. These facts will determine the maximum concentration of active intermediates and consequently the maximum of activity.

Key words: NO_x-SCR mechanism, propene, Pt-beta catalyst, transient experiments.

1. Introduction

Numerous papers deal with the study of the mechanism of NO_x reduction by hydrocarbon in the presence of excess oxygen on platinum based catalysts. However there is no evidence that allows defining a single reaction path. Pt/Al₂O₃ and Pt/SiO₂ catalysts have been the most studied catalytic systems and therefore, those about which more is known. One of the conclusions arising from a detailed study of the literature is the different reaction paths for different hydrocarbons, as it appears when comparing propane and propene [1]. The Pt oxidation state is a key issue in determining the reaction mechanism and this seems to be related to the different nature of the hydrocarbon-metal bond [2-4]. Much less attention has been paid to the study of the reaction mechanism over Pt-zeolite based catalysts [5], although the effect of the hydrocarbon seems to be similar as in non-zeolitic systems. In order to study the reaction mechanism over Pt-zeolite catalysts a single hydrocarbon must be selected and propene has been considered to be the model hydrocarbon for this reaction.

In the literature, two types of reaction mechanisms have been proposed:

i) Reaction intermediates from partial hydrocarbon oxidation

This mechanism is based on the active role of certain species derived from the partial oxidation of the hydrocarbon. Several authors claim that some deposits appearing on the catalyst during the NO/C₃H₆/O₂ reaction play an important role in the reaction, because they are the source of very reactive radical species able to take part as reaction intermediates in some reaction steps [6,7]. Pt phase might catalyze the formation of these carbonaceous deposits either by cracking or partial oxidation of the hydrocarbon, thus, generating a large amount of allyl groups [8,9], carbenium ions [10], groups such as –CN and –NCO [11-17]etc., that will then react with oxidizing species (NO, NO₂, O₂) yielding the reaction products (N₂, N₂O, CO₂).

Others authors [12,18-24] propose a path based on the formation of NO₂ which reacts with propene to form different reaction intermediates. Most of them consider these intermediates to be organo-nitro and organo-nitrite species, although others [23] propose other partially oxidized intermediates such as γ -hydroxynitropropane. Recently, Duprez et al [25] investigate the reactivity of several compounds with different organic functions with the aim to explore their potential role as intermediates in the NO reduction. They come to the conclusion that oxime species should play a key role in the NO_x reduction by alkenes at temperatures below 250 °C. Oximes are tautomeric forms of nitroso compounds. An interesting point of this study is the explanation of N₂O and N₂ formation through the Nef and Beckmann reactions,

respectively. The oxime route was previously proposed by Garin and co-workers [26-28].

ii) *Catalytic decomposition of NO and regeneration (reduction) of the active sites by hydrocarbon.*

This is basically a redox mechanism in which, after dissociative chemisorption of NO and desorption of N₂ and/or N₂O, the hydrocarbon reacts with adsorbed oxygen (O_{ads}) on the catalyst. This mechanism, initially proposed by the group of Iwamoto [29], has been deeply investigated by Burch's group [1, 30-33], and several authors support it as no evident proof has been found to support the other proposed mechanisms [17,34].

Finally, the possibility of a mixed reaction mechanism, in which some steps of the previous described mechanism take place, cannot be ruled out. In fact, Burch, in one of his most recent papers [1], indirectly recognizes that the presence of certain intermediates coming from the activation of the hydrocarbon can fit into the mechanism proposed by his group.

Considering the controversial situation described, this work deals with the study of the NO/C₃H₆/O₂ reaction over Pt-zeolite based catalysts with the objective of finding evidence of the reaction steps involved. For that, a Pt-beta sample, whose catalytic behavior has been thoroughly investigated [35], has been selected. Non-isotopic transient analysis techniques have been used as experimental methodology, as these techniques have been proved to be a valuable source of information in the study of Pt/Al₂O₃ and Pt/SiO₂ systems [36]. The experiments have been designed to provide answers to the volcano-type activity behaviour of the catalytic system.

2. Experimental.

A Pt-beta catalyst (Pt-beta(r-0.5)) has been selected to study the reaction mechanism of the NO/C₃H₆/O₂ reaction by means of transient analysis techniques. Details on the preparation and characterization of this catalyst can be found elsewhere [35]. As a summary, this catalyst has been prepared by aqueous ion-exchange of beta-zeolite with a 3·10⁻⁴ M aqueous solution of the metal precursor ([Pt(NH₃)₄](NO₃)₂). After successive ion-exchange experiments (20°C during 18 hours) a catalyst with a 1 wt. % metal content is obtained. The exchanged zeolite is filtered, washed with de-ionized water and dried at 110°C for 12 hours. Finally, it is calcined at 400 °C during 2 hours and reduced at 350°C in pure H₂ atmosphere during 8 hours, using a heating rate of 0.5°Cmin⁻¹.

Figure 1 shows the scheme of the experimental device used in the kinetic analysis experiments. The gas control panel consists of six mass flow controllers (d) (0.1 ml/min sensitivity). A four-way electro valve (c) allows automatically switching two of the gas streams. To avoid altering the total pressure of the system, a high precision regulation valve (m) has been introduced in the system. The pressure of the gas streams is controlled by means of two high-sensitivity pressure transducers (j) (0-0.6 mbar). The outlet of the gas control panel is connected to the reaction system, which consists of a tubular quartz reactor ($\varnothing=5$ mm) (e) and a horizontal furnace (f). Temperature is controlled with a sensitivity of 0.1°C/min (h) and monitored by two thermocouples (g). The outlet of the reactor is connected to the gas analysis system, a mass spectrometer (Pfeiffer OmniStar, sensitivity 0.1 s) (n).

By using this experimental device, two different sets of experiments have been carried out:

i) Steady State transient switch: The relaxation of the system is analysed when it is subjected to some selected switches in which a reagent is suddenly eliminated from the system and an inert gas (Ar) replaces it, avoiding changes in temperature and pressure. The inverse switch, i.e. reintroducing the reagent, is also a valuable source of information. Thus, $C_3H_6/NO/O_2 \rightarrow C_3H_6/Ar/O_2$, $C_3H_6/Ar/O_2 \rightarrow C_3H_6/NO/O_2$; $C_3H_6/NO/O_2 \rightarrow Ar/NO/O_2$, $Ar/NO/O_2 \rightarrow C_3H_6/NO/O_2$; $C_3H_6/NO/O_2 \rightarrow C_3H_6/NO/Ar$ and $C_3H_6/NO/Ar \rightarrow C_3H_6/NO/O_2$ switches have been carried out and analysed. In order to develop a mechanistic study by means of this technique, it has to be kept in mind that the conversion levels must be kept lower than 25%, in order to ensure differential reaction conditions [37]. Therefore, these experiments were not carried out at the temperature of the maximum of activity (T_{max}) but at lower temperatures, usually 20°C lower. The kinetic study at temperatures higher than that corresponding to the maximum activity, even though not yielding precise information about reaction mechanism (hydrocarbon conversion is always 100%) can be of interest to know more about the state of the catalyst under those conditions.

All experiments were carried out at atmospheric pressure with a total flow of 150 ml STP/min and 0.13 g of catalyst (space velocity=50000 h⁻¹). The reaction stream contains 2262 ppm NO, 3400 ppm C₃H₆ and 5% O₂ in He. The inert gas stream is 1% Ar in He. Data corresponding to the switching experiments have been mathematically normalised between 0 and 1, in order to make the analysis easier, using the following equations:

$$(a) \text{ Species that increase its concentration: } Rn_x = \frac{C_x - C_{i,ss}}{C_{f,ss} - C_{i,ss}}$$

(b) Species that decrease its concentration: $Rn'_x = \frac{C_x - C_{f,ss}}{C_{i,ss} - C_{f,ss}}$

where: Rn_x y Rn'_x : normalized response of "X", C_x : absolute concentration of 'x', $C_{i,ss}$: initial concentration in the steady state, $C_{f,ss}$: final concentration in the steady state.

ii) Thermal Programmed Desorption (TPD): After reaction, the sample is treated with an inert gas flow (100 ml STP He/min) while the temperature is gradually increased at a constant rate (5°C/min). The evolution of different gases, followed by mass spectrometry, allows obtaining information about the nature and stability of the species present on the catalyst surface.

3. Results

Figure 2 shows the NO_x and C_3H_6 conversion profiles as a function of temperature as well as the NO_2 evolution profile for the Pt-beta catalyst obtained in the experimental system described in reference [35] but in the same experimental conditions used in the mechanistic study discussed in this paper. The NO_x conversion curve presents the typical trend observed for Pt catalysts [35], a well defined maximum of activity at the same temperature where the maximum hydrocarbon conversion is achieved. The N_2 selectivity between 175 to 350 °C has a constant value of 35%. At higher temperatures, NO_2 evolution is observed but its concentration change with temperature due to kinetics and thermodynamic limitations. The maximum NO_x conversion level achieved by this catalyst is slightly lower than the previously observed [35] due to the experimental conditions used in this study (higher space velocity).

The temperatures for the switch experiments have been selected according with the results shown in Figure 2. Considering that the maximum activity is achieved at 220°C (T_{max}), 200°C and 230°C have been used to carry out the experiments below and above T_{max} .

3.1 Transient analysis experiments below T_{max} (200°C)

The transient analysis experiments were conducted after the $C_3H_6/NO/O_2$ reaction steady state conditions were reached at 200 °C. Under these conditions, the NO and C_3H_6 conversions were 19 and 17 %, respectively.

3.1.1. $C_3H_6/NO/O_2 \leftrightarrow C_3H_6/Ar/O_2$ switch.

Figure 3 shows normalised response of the Pt-beta catalyst when NO is replaced by Ar at 200°C. It can be observed that normalised NO profile is the same as downstep Ar response (Ar⁻¹ from now) profile, indicating that reversible adsorbed NO on the Pt surface is practically zero at the studied reaction temperature.

Propene also shows the same profile although it is delayed compared to Ar⁻¹. It is worth noting that hydrocarbon is only partially consumed at 200°C (see Figure 2), so when the switch takes place, the decrease of propene concentration is due to its combustion by oxygen present in the reaction system. This behaviour reveals that, under usual reaction conditions and, even though the large excess of oxygen ($O_2/C_3H_6 > 30$), the combustion of propene is disfavoured. To explain this result, the hypothesis of Xin et al [38] suggesting a direct competition between NO and O₂ for Pt surface sites has been used. This competition is in favour of NO at temperatures below the temperature of T_{max}. Also, Garin [28] support this hypothesis which is in accordance with the fact that, at low temperature, the sticking coefficient of NO (σ_{NO}) is higher than the oxygen one (σ_{O_2}) [39,40] and, when temperature increases, σ_{NO} decreases and σ_{O_2} increases. The delay in the propene profile indicates that there are enough NO_{ads} species on the catalyst surface to ensure that the NO reduction reaction continues, for a few seconds, even in the absence of NO in the gas phase. When this NO is reduced (by propene), the adsorption free sites formed, can now be occupied by oxygen that will dissociate generating O_{ads} species in a slow process. This sequence of events is in agreement with the mechanism proposed by Burch et al. [2], in which an “induction time” for hydrocarbon combustion, related to a slow dissociative adsorption of O₂ and/or its slow reaction with adsorbed hydrocarbon, is proposed.

The O₂ profile also presents a delay with respect to Ar⁻¹. This delay is approximately of the same magnitude as that observed for propene, confirming that oxygen is replacing NO on adsorption sites. The oxygen signal shows a minimum. This is an indication of an extra demand of oxygen with respect to steady state. This additional demand is due to the fact that not only the hydrocarbon from the reaction stream is being consumed, but also the hydrocarbon adsorbed on the catalyst surface. The amount of adsorbed hydrocarbon must be high, as can be deduced from the O₂ signal response. The excess of CO₂ shown in Figure 3 coincides, in time, with the minimum in the oxygen signal, supporting the hypothesis of a rich hydrocarbon surface. Burch et al. [36], using Pt/Al₂O₃ and Pt/SiO₂ catalysts, observed at temperatures below the maximum of activity, and independent of the support used, that the catalyst surface is mainly covered by hydrocarbon derived species.

As a summary, the study of the relaxation of the NO/C₃H₆/O₂ system during a C₃H₆/NO/O₂ → C₃H₆/Ar/O₂ switch, allows inferring that at 200°C, a high proportion of

adsorbed hydrocarbon exists on the catalyst surface. This situation arises as a consequence of preferential adsorption of NO over O₂ on Pt active sites, thus inhibiting hydrocarbon combustion. All these facts explain why hydrocarbon is consumed by the reduction of NO, as expected for a highly selective system, and not by its reaction with oxygen.

Figure 4 shows the results of the inverse switch (C₃H₆/Ar/O₂ → C₃H₆/NO/O₂) at 200°C for the same catalyst. When steady state is reached, NO reduction is again the preferential reaction. The recovery of the initial situation necessarily implies that NO adsorption on Pt is preferential over O₂ adsorption on Pt. NO and O₂ profiles are practically identical confirming their relationship: NO adsorbs on sites left free by oxygen (O_{ads}) when are consumed by combustion of adsorbed hydrocarbon species.

It is important to point out that recovering the initial state the system follows two different kinetics (see Figure 4 inset). All reactants and products present a profile with two clearly different slopes. Initially, NO reduction is fast recovered but it slows down 5 seconds after the switch. The system goes back to the initial levels of conversion. This seems to indicate that two different types of Pt sites are present on the catalyst. This could be related to the fact that two different Pt particle sizes may exist in the sample. Considering that the energy of the bond Pt-O_{ads} in small Pt clusters is greater than in large Pt clusters [38], reduction of O_{ads} species during hydrocarbon combustion must be more favourable in large Pt particles. In this sense, TEM results reveal that two different Pt particle sizes are present on Pt-beta catalysts. The main fraction is ca. 2nm although larger particles are also found (ca. 50 nm) [35]. Thus, when NO is reintroduced in the system, the first fast kinetics stage would correspond to the formation of NO_{ads} species in large Pt particles, where O_{ads} species are easily reduced. The second stage, clearly being a slower process, would also correspond to formation of NO_{ads} but in more abundant small Pt particles, where O_{ads} is strongly bound to the Pt surface. These observations are in direct relation with the structure sensitivity character of the Pt-catalysed NO/C₃H₆/O₂ reaction demonstrated elsewhere [35]. However the existence of different sites on the Pt particles (surface heterogeneity) can not be rejected.

In Figure 4, it is apparent that CO₂ signal decreases immediately after the switch as a consequence of the partial inhibition of hydrocarbon combustion, indicating that O_{ads} reduction in large Pt particles is a fast process. The propene profile shows a delay of 2 seconds evidencing a fast covering of the catalyst surface with C₃H₆ species (These species cover the surface of the catalyst during NO reduction as previously discussed in the C₃H₆/NO/O₂ → C₃H₆/Ar/O₂ switch at 200°C).

Finally, it is of interest to note that, in the $C_3H_6/Ar/O_2 \rightarrow C_3H_6/NO/O_2$ switch, no NO_2 is released to the gas phase when NO is introduced to the system, even though the Pt surface is mainly covered by O_{ads} species. The NO_{2ads} could exist in the surface of Pt particles but it is not release to the gas phase up to higher temperatures as it will be shown later. This idea is confirmed by a very recent publication [41].

3.1.2. $Ar/NO/O_2 \leftrightarrow C_3H_6/NO/O_2$ switch.

Figure 5 shows the response of the system to the elimination of reductant at 200°C. C_3H_6 profile is the same as the Ar^{-1} profile, showing that the surface coverage of C_3H_6 reversibly chemisorbed species is practically zero. In the absence of C_3H_6 , the only reactive species are NO and O_2 , therefore formation of NO_2 should be favoured, however no NO_2 in the gas phase is detected. The fact that the oxygen concentration does not vary during the switch (not shown in Figure 5) is also in accordance with this. The NO signal shows a delay of several seconds with respect to Ar^{-1} , showing that NO reduction continues during this period of time even in the absence of the hydrocarbon. The $C_3H_6/NO/O_2 \rightarrow C_3H_6/Ar/O_2$ switch discussed above has provided enough evidence of the existence of a hydrocarbon rich surface at 200°C, and this may account for the fact that NO reduction continues when propene is not present in the gas phase. The vacant sites formed when C_3H_{6ads} species react, are now being occupied by NO_{ads} accounting for the extra time that NO needs to reach the steady state.

The existence of C_3H_{6ads} species on the catalyst surface is also supported by the CO_2 profile (combustion product), which shows two different combustion kinetics. When C_3H_6 is eliminated, a rapid consumption of hydrocarbon becomes favoured as indicated by the CO_2 signal profile, which starts to rise immediately after the switch, reaches a maximum and decreases slowly to zero (not shown in Figure 5). During the fast combustion stage, C_3H_6 species located on (or close to) the active phase is involved. In addition, hydrocarbon species located on the support must exist. These species have to migrate towards the active phase to reach Pt sites or spillover of adsorbed NO from Pt to the support, should occur giving rise to a slower combustion process. These processes are unlikely to occur during steady state reaction conditions as propene is continuously fed into the system. Related to this, it is apparent from Figure 5 that NO and CO_2 signals take different time to reach the new steady state, indicating that under reaction conditions, not all propene present on the catalyst surface (Pt+zeolite) is involved in the reduction of NO, being the active species those located on the active phase and not on the support.

Elimination of C_3H_6 leaves the surface in an oxidised state. Figure 6 shows the normalised profiles of the most important species during the $Ar/NO/O_2 \rightarrow C_3H_6/NO/O_2$ switch performed on the Pt-beta catalyst at 200°C. The CO_2 signal rises immediately after the introduction of propene to the system. This can only be justified if the surface was covered with O_{ads} (created by dissociation of NO_{ads} in the absence of C_3H_{6ads}). According to Burch et al. [2], the reaction between propene in the gas phase and adsorbed oxygen is a fast process. This sequence also explains the delay shown in the propene signal.

The NO profile is reverse to that of CO_2 . To understand the relationship between these two species, it must be considered that when hydrocarbon is reintroduced into the system, it reacts with O_{ads} species, liberating a large amount of Pt sites which are immediately occupied by NO until the steady state, where NO reduction recovers its initial values, is achieved. The oxygen level (not shown in the figure) remains constant during the switch. These results evidence, again, the direct competition between NO and O_2 for Pt free sites. At temperatures lower than T_{max} , this competition is very much in favour of NO, and therefore NO reduction selectively takes place over hydrocarbon combustion.

3.1.3. $C_3H_6/NO/O_2 \leftrightarrow C_3H_6/NO/Ar$ switch.

Figure 7 shows the response of the system to a $C_3H_6/NO/O_2 \rightarrow C_3H_6/NO/Ar$ switch. The O_2 profile indicates that oxygen is also irreversibly adsorbed on the catalyst surface or simply that it is not adsorbed at all. When oxygen is eliminated from the system, CO_2 evolution ceases immediately, indicating that O_2 is essential for the reaction to occur and that O_{ads} coverage at this temperature is very low, as the reaction does not continue in the absence of this gas. This agrees with recent results of Duprez and co-workers [25].

The fact that propene and NO profiles are identical indicates that the catalyst surface accepts both species proportionally up to 150 seconds after the switch, when saturation of the surface occurs. After the switch, both molecules are adsorbing on the catalyst to the same extent as they did under usual reaction conditions, although slower kinetics of adsorption are observed. Considering these facts, it can be assumed that NO and C_3H_6 are involved in the generation of partially oxidised hydrocarbon species through a slow reaction. This species may have an important role on the reaction, as has been put forward by other authors [6,7, 25-28]

From these results, it could be concluded that adsorption of hydrocarbon on Pt is followed by a reaction in which NO_{ads} and C_3H_{6ads} would participate to form partially oxidized hydrocarbon species. In these conditions, the surface is covered by these

species that need the action of oxygen gas to react completely to CO_2 and liberate Pt free sites for the reaction to continue. When O_2 is not present in the system, the surface of the catalyst is covered by partially oxidised hydrocarbon species producing catalyst deactivation.

Figure 8 shows the response of the system when O_2 is reintroduced at 200°C . This switch also needs longer times to reach steady state. Right before the switch, the surface is covered by NO_{ads} , $\text{C}_3\text{H}_6_{\text{ads}}$ and oxidised hydrocarbon species as will be shown later. The CO_2 profile rises immediately after the switch. As O_2 adsorption is a slow process at this temperature [2], the fast CO_2 evolution must be the result of the reaction between gas phase oxygen and partially oxidised hydrocarbon species in a fast reaction.

NO and C_3H_6 profiles are again identical as they adsorb in the same proportion to produce new partially oxidised hydrocarbon species.

The O_2 profile presents a maximum right after the switch is performed. The overshoot means that there is a very short period of time where oxygen cannot chemisorb or react, and then this situation changes towards an oxygen consumption that establishes the new steady-state.

3.1.4. Temperature Programmed Desorption of Pt-beta catalyst after reaction at 200°C .

Figure 9 shows the evolution of different compounds from the catalyst surface after 10 hours under $\text{NO}/\text{C}_3\text{H}_6/\text{O}_2$ reaction conditions at 200°C . First of all, a very important propene evolution can be observed starting at 230°C and reaching a maximum at 325°C . TPD experiments after adsorption of C_3H_6 on zeolite beta give similar propene peak. It is believed that these hydrocarbons molecules exists in the catalyst support, as previously mentioned, but probably are not involved in the NO reduction reaction.

The absence of NO in Figure 9 indicates the irreversible adsorption of these species under reaction conditions at 200°C . This supports the hypothesis of NO_{ads} species react with $\text{C}_3\text{H}_6_{\text{ads}}$ species to form partially oxidised hydrocarbon species. The absence of O_2 in Figure 9 indicates that O_{ads} species does not combine to form O_2 .

CO_2 , N_2 , and N_2O are desorbed from the surface in a much lower concentration than propene and the evolution of these gases may be the result of decomposition of partially oxidised hydrocarbon species. In this line, Praserthdam et al. [24] have investigated the formation of these intermediates on $\text{Pt}/\text{Al}_2\text{O}_3$ catalysts finding TPD profiles similar to those shown in Figure 9, except that the C_3H_6 peak is not present in their experiments due to the low propene adsorption capacity of the Al_2O_3 support. Praserthdam et al. suggest that $\text{C}_x\text{H}_y\text{O}_z\text{N}_w$ and $\text{C}_x\text{H}_y\text{O}_z$ intermediates may be present

on the catalyst surface. This study gives no evidences of two types of intermediates and, it is proposed $C_xH_yO_zN_w$ as a general formula.

TPD experiments after reaction at 200°C seem to agree with the hypothesis of a step in which adsorbed hydrocarbon reacts with adsorbed NO to form $C_xH_yO_zN_w$ during the reaction of NO with propene under oxidising conditions.

3.2. Transient analysis experiments above T_{max} (230°C)

The transient analysis experiments were conducted after the reaction steady state conditions were reached at 230 °C. As was previously stated, in order to perform a non-isotopic switch study, the system must be under differential reaction conditions. In the NO/C₃H₆/O₂ reaction at temperatures higher than T_{max} , these conditions are not fulfilled, the hydrocarbon conversion is always 100% making these type of studies as well as the interpretation of the results very difficult. However, it is possible to extract valid information on how the catalyst behaves under these circumstances. To make discussion simpler, only those experiments which have provided relevant information will be presented here.

3.2.1 C₃H₆/NO/O₂ ↔ C₃H₆/Ar/O₂ switch.

Figure 10 shows the most relevant profiles of reactants and products during the relaxation of the Pt/beta system, after NO is eliminated from the feed at 230°C. Three main differences are observed when comparing with the situation at 200°C (Figure 3).

First of all, there is not propene profile. At 230°C and before the switch, hydrocarbon conversion is 100% and, the NO_x conversion is 65%. According to this, C₃H_{6ads} coverage must be very low. After C₃H₆/NO/O₂ → C₃H₆/Ar/O₂ switch, hydrocarbon conversion is also 100% indicating that the fraction of hydrocarbon that participates in the reduction of NO before the switch is immediately burnt with oxygen after the switch, suggesting that at this temperature the O_{ads} coverage is much higher than at 200 °C, as a consequence of the low coverage of C₃H_{6 ads} species and the favoured dissociation of oxygen by the temperature increase, even in the presence of NO.

Secondly, the NO profile decays slowly after the switch. This behaviour is an indication that certain equilibrium between NO in the gas phase and adsorbed NO is being established. Since an increase in temperature would be unfavourable for the NO adsorption, the process should occur through the formation of different species as will be described follow on.

The third difference is in the oxygen profile, there is a minimum that occurs at the same time as the maximum of the CO₂ profile. The evolution of CO₂ starts

immediately after the NO switch. It seems that some species at the surface are burnt more easily in the absence of NO. However, the O₂ signal shows a progressive increase until it reaches the final level, corresponding to the fraction used to burn the hydrocarbon in reaction conditions. During the reaction, there must exist another process of oxygen consumption that ceases when NO is eliminated. The only possible explanation is that during the reaction at 230°C, some NO is being oxidised to NO₂; in fact Figure 2 shows that NO₂ evolution occurs after the maximum of activity, confirming this hypothesis. The existence of NO_{2ads} could be the origin of NO in gas phase following reaction (1).



When NO is introduced back into the system (C₃H₆/Ar/O₂ → C₃H₆/NO/O₂), the previous situation is not recovered, i.e. there is no activity for the NO reduction reaction. The C₃H₆/NO/O₂ ↔ C₃H₆/Ar/O₂ switch at temperatures higher than T_{max} is therefore an irreversible switch. The reason for this deactivation may be the lack of reaction between NO_(g) and O_{ads} which will cover the active sites under these conditions. The deactivation also can be produced by the formation of carbonaceous deposits coming from the incomplete combustion of the hydrocarbon. The formation of these deposits that do not cause catalyst deactivation at T_{max} was already observed and studied in detail elsewhere [35]. It seems that in the C₃H₆/NO/O₂ → C₃H₆/Ar/O₂ switch, the absence of NO and the high temperature used favours the formation of these deposits that are stable at 230 °C even in the presence of oxygen. These deposits block the surface of the catalyst, inhibiting the adsorption of NO and, as a consequence, its oxidation to NO₂ or its reduction with propene. The absence of NO₂ evolution during the switch supports this explanation. As NO adsorption does not take place when this type of deposits are present [36], the re-introduction of NO does not achieve the recovery of the system to its initial state where NO reduction was the most important reaction. On the contrary, hydrocarbon combustion is not affected at all.

It seems feasible that one of the roles of NO₂ is the elimination of coke deposits from the active phase preventing catalyst deactivation. In order to check the hypothesis about the role of NO₂, a new switch at 230°C was carried out, after 10 hours in reaction conditions (2262 ppm NO, 3400 ppm C₃H₆ and 5% O₂ in He), the NO was eliminated (C₃H₆/NO/O₂ → C₃H₆/Ar/O₂ switch) and, subsequently, C₃H₆/Ar/O₂ was switched by C₃H₆/NO₂/O₂. The profiles shown in Figure 11 confirm our hypothesis. Note that the

NO₂ is consumed by reaction with coke deposits as indicates the concomitant evolution of CO₂.

3.2.2. Ar/NO/O₂ ↔ C₃H₆/NO/O₂ switch

The elimination of the reductant from the system, at 230 °C, induces an increase in the NO₂ concentration. This is the unique conclusion extracted from the C₃H₆/NO/O₂ → Ar/NO/O₂ switch. In contrast to this, the elimination of the reductant at temperatures lower than T_{max} (200°C) did not originate NO₂ evolution. This difference can be explained by the high O_{ads} coverage that exists at temperatures higher than T_{max}.

The Ar/NO/O₂ → C₃H₆/NO/O₂ switch at 230°C is shown in Figure 12. This is a reversible switch, i.e. after the switch the system goes back to its initial situation. However, in the relaxation time, it can be observed how NO₂ concentration increased in the previous switch (C₃H₆/NO/O₂ → Ar/NO/O₂) decreases together with Ar and reaches a minimum before increasing again until the stationary state. The drop of the NO₂ profile after the introduction of propene to the system is an obvious consequence of the reaction of NO_{2ads} with the hydrocarbon.

CO₂ shows a rapid evolution during a few seconds after propene is introduced and, later the profile presents a change in slope until it slowly reaches the stationary state. The fast evolution of CO₂ after the switch is indicative of a fast reaction between NO_{2ads} species and C₃H₆ in either the gas phase or through a fast adsorption leading to hydrocarbon fragments, i.e. a fast combustion of the first propene molecules.

O₂ and NO present a similar profile after hydrocarbon is fed back into the system. The concentration of these reactants decreases with fast kinetics and then the kinetics slow down. NO and O₂ concentrations decrease as they adsorb on free Pt sites whose are being generated during hydrocarbon combustion.

3.2.3. Temperature Programmed Desorption of Pt-beta catalyst after reaction at 230°C.

Figure 13 shows the results of temperature programmed desorption experiment carried out with Pt-beta catalyst after 10 hours under reaction conditions at 230°C. First of all, it must be noted that propene evolution is not observed in the whole range of temperature studied, indicating that molecular propene is not stored in the catalyst (Pt+zeolite) after the maximum of activity. In Figure 9, desorption of hydrocarbon was shown to begin at 220°C, and this justifies the fact that at 230°C the hydrocarbon cannot adsorb on the catalyst. This does not imply that hydrocarbon fragments are not present.

Although NO_2 has been detected in the gas phase during the reaction at 230°C (see Figure 2), no evolution of this gas is observed during the TPD experiment showing that this molecule is not adsorbed under reaction conditions. Therefore this species as soon as it forms either reacts (as we have proposed for coke deposits) or evolves rapidly from the surface.

The profiles of CO_2 and N_2 are very similar to those shown in Figure 9 (TPD after reaction at 200°C). A clear difference is the absence of N_2O .

The CO_2 signal presents a peak at ca. 260°C probably arising from the reaction of carbonaceous deposits, formed during the reaction. The absence of H_2O (not shown in the figure) in this temperature interval, make us think that the carbonaceous deposits are coke-like deposits instead of species coming from the adsorption of hydrocarbon on the catalyst surface ($\text{C} + \text{O}_2 \rightarrow \text{CO}_2$), probably produced by the propene cracking. Considering the area of the peak we deduce that the formation of these deposits is low although not negligible. Based on the temperature at which this peak appears, the coke deposits must grow on the surface of the active phase or close to it [42,43].

Oxygen shows an interesting profile. There is an important desorption of oxygen at the temperature of the reaction, confirming that O_{ads} coverage is very important on the catalyst surface. Desorption is followed by an oxygen consumption up to 260°C , temperature at which coke combustion takes place. This fact supports the hypothesis of an important amount of oxygen adsorbed on the catalyst surface at temperatures higher than T_{max} , being able to oxidise the coke deposits formed on the catalyst even during a treatment under inert atmosphere (TPD).

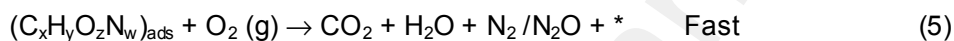
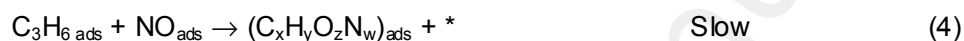
4. Discussion

4.1. The state of Pt-beta catalyst at temperature below T_{max}

At temperatures below T_{max} , the surface of the Pt-beta catalyst is mainly covered by adsorbed hydrocarbon species. An important fraction of which is adsorbed on the zeolite support. On the contrary O_{ads} coverage is very low under these reaction conditions.

Considering the information on the state of the catalyst surface, it seems that there exists a direct competition between NO and O_2 for Pt adsorption sites, being favourable to NO . The dissociative chemisorption of oxygen is not favoured, and as a consequence, the combustion of the hydrocarbon permits the selective reduction of NO even in an $\text{O}_2/\text{NO} > 45$. These conclusions agree with those obtained by Burch et al. [32] using Pt/SiO_2 and $\text{Pt}/\text{Al}_2\text{O}_3$ catalysts. In addition, this study allows us to conclude

that the reaction between NO and propene is not a direct reaction, but it goes through a series of intermediates of composition $C_xH_yO_zN_w$ formed from NO_{ads} and C_3H_{6ads} . These intermediates could be identified as the “active radicals” that Obuchi et al. [6] and Ansell et al. [7] described in their works. Jeon et al. [44,45] have also observed the active role of surface carbon species in the reduction of NO by propene when using Pt/VMCM-41 catalysts. The coverage of the active phase by these intermediates is not high due to their high reaction rate with oxygen in the gas phase. Therefore, the role of oxygen is the combustion of these intermediates to leave free Pt sites for the adsorption of NO and C_3H_6 assuring the course of the reaction. The next reaction sequence summarises the global process that takes place before the maximum of activity.



(*: indicates active Pt sites (free and reduced) for the adsorption of reactants).

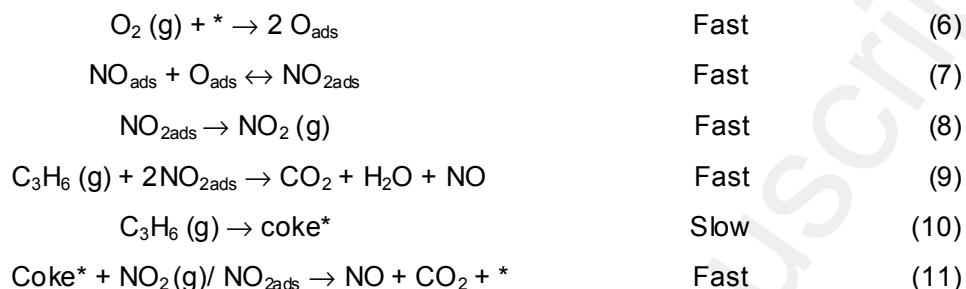
The reaction takes place through the adsorption of NO on a free reduced Pt (reaction (2)), this step seems to be fast at least in some of the Pt particles (see Figure 4).

If only NO exists in the gas phase, the catalyst surface would be progressively covered by NO_{ads} species, and the catalyst would completely deactivated. Therefore, the presence of a reductant is needed in order to eliminate these species. To do so, the hydrocarbon must, first of all, adsorb on the surface of the catalyst, in a fast reaction (reaction (3)) [36]. The regeneration of Pt active sites goes through some partially oxidised hydrocarbon species which form through reactions (4). This reaction seems to be slow (see Figure 7). The formation of these intermediates, which can be seen as an activation of the hydrocarbon, has been put forward by several authors [6,7, 25-28, 44,45]. The complete oxidation of these intermediates with oxygen in the gas phase (reactions (5)) is a fast process (see Figure 8) which creates, again, active Pt sites closing the catalytic cycle.

4.2. The state of Pt-beta catalyst at temperature above T_{max} .

The surface of the Pt-beta catalyst at temperatures higher than T_{max} is mainly covered by O_{ads} species because, at this temperature, the dissociation of oxygen is

faster than at 200 °C. The concentration of adsorbed hydrocarbon on the active phase or the zeolite support over the maximum of activity is very low. The higher temperature also favours the formation of carbonaceous deposits probably by the propene cracking that nevertheless do not imply the deactivation of the catalyst. NO₂ plays a fundamental role in the reaction. The state of the catalyst surface favours NO₂ formation, keeping the active phase free of coke deposits, that otherwise would deactivate the catalyst. The next sequence summarises the additional reactions, besides (2), (3), (4), (5) occurring in the global process at temperatures above T_{max}.



The net change in the reaction mechanism when temperature is higher than T_{max} is motivated by the fast dissociative adsorption of the oxygen molecule on the metal surface (reaction (6)) that leads to a high coverage of O_{ads} species on the catalyst surface facilitated by the absence of C₃H_{6ads} and the increase in temperature. These species react with NO_{ads} to yield NO_{2ads} (reaction (7)). NO_{2ads} reacts with the propene in the gas phase (reaction (9)), or can be desorbed to form NO₂(g) (reaction (8)). The high reactivity of NO₂ leads to the fast reaction with coke deposits (formed by reaction (10)) through reaction (11). Reactions (9) and (11) give NO as NO₂ reduction product [46,47], consequently when these reactions become important, the NO reduction activity decreases

Shen and Kawi [48] found a change in kinetic from surface reaction controlled to external mass transfer controlled at the temperature of the maximum activity using Pt/MCM-41 catalyst. Below the maximum, the surface reaction is suggested to be slow and becomes the controlling step for the overall NO conversion reaction. Above the maximum, the activation of C₃H₆ is very fast and reaches complete oxidation. Although the mass transfer rate is faster at higher temperature, however the rate of surface reaction may exceed the rate of external mass transfer of reactant. In our system a similar behaviour was found [49].

4.3. State of the Pt-beta catalyst at the maximum of activity.

The NO and C₃H₆ conversions at the maximum of activity are very high, see Figure 2. This fact invalidates the use of transient analysis techniques to determine the

state of the catalyst and, as consequence, the reaction mechanism. It is reasonable to think that the situation must be a transition between the two previously described situations. Before the maximum of activity, the catalyst surface is mainly covered by C_3H_{6ads} species resulting in an essentially reduced metal phase. After the maximum of activity, the high coverage of O_{ads} species results in a mainly oxidised metal phase.

The oxidation state of Pt during the $NO/C_3H_6/O_2$ reaction at the maximum of activity has been previously studied by X-Ray Photoelectron Spectroscopy (XPS) [35]. Results reveal that at the maximum of activity Pt(0) and Pt(II) coexist which is in agreement with the hypothesis of presenting the situation at the maximum of activity as a transition between the Pt surface situation before the maximum (Pt(0)) and after the maximum (Pt(II)).

The transient analysis studies performed at temperatures lower and higher than the maximum of activity allow to draw the following scenario for the steps occurring at the catalyst surface. NO must adsorb on the surface of Pt and form NO_{ads} species. The adsorption of propene also takes place at the catalyst. The reaction proceeds through the slow formation of partially oxidised active intermediates ($C_xH_yO_zN_w$). The combustion of the intermediates with $O_2(g)$ is the main step cleaning the Pt active sites so the reaction can continue. Temperature has a positive effect on the surface reaction producing active intermediates. On the contrary, formation of NO_{ads} and C_3H_{6ads} are not favoured by an increase in temperature. This fact will determine the maximum concentration of active intermediates and consequently the maximum of activity.

5. Conclusions

The transient analysis study of the selective reduction of NO_x with propene on Pt-beta catalyst provides insights to better understand the mechanism of the reaction and the changes occurring at the maximum of activity.

- A direct competition between NO and O_2 for Pt adsorption sites exists, being favourable to NO. The dissociative chemisorption of oxygen is not favoured, and as a consequence, the combustion of the hydrocarbon permits the selective reduction of NO.
- The reaction proceeds through the slow formation of partially oxidised active intermediates ($C_xH_yO_zN_w$) formed from NO_{ads} and C_3H_{6ads} . The combustion of the intermediates with $O_2(g)$ is the main step cleaning the Pt active sites.
- Temperature will determine the maximum concentration of active intermediates because has a positive effect on the surface reaction producing active intermediates, but, a negative effect on the formation of NO_{ads} and C_3H_{6ads} .

- The high reactivity of NO₂, favoured at temperatures above T_{max}, produces the consumption of the hydrocarbon without NO reduction and consequently the decrease in activity.

Acknowledgments

The authors thank the Spanish Ministry of Education and Science (project CTQ2005-01358) for the financial support.

References

- [1] R. Burch, J. P. Breen y F. C. Meunier, *Appl. Catal. B*, 39 (2002) 283.
- [2] R. Burch and T. C. Watling, *J. of Catal.* 169 (1997) 45.
- [3] M. C. Demicheli, L. C. Hoang, J. C. Menézo and J. Barbier y M. Pinabiau-Carlier, *Appl. Catal. A*, 97 (1993) L1.
- [4] R. Burch, P. Fornasiero, T. C. Watling, *J. Catal.* 176 (1998) 204.
- [5] Y. Traa, B. Burger y J. Weitkamp, *Micropor. Mesopor. Mater.* 30 (1999) 3.
- [6] A. Obuchi, A. Ogata, K. Mizuno, A. Ohi, M. Nakamura, H. Obuchi, *J. Chem. Soc. Chem. Commun.* (1992) 247.
- [7] G. P. Ansell, A. F. Diwell, S. E. Golunski, J. W. Hayes, R. R. Rajaram, T. J. Truex, A. P. Walker, *Appl. Catal. B*, 2 (1993) 81.
- [8] G. J. Buckles, G. J. Hutchings, *J. Catal.* 151 (1995) 33.
- [9] N. W. Hayes, R. W. Joyner, E. S. Shpiro, *Appl. Catal. B*, 8 (1996) 343.
- [10] G. A. Somorjai, *Introduction to Surface Chemistry and catalysis*, John Wiley & Sons Eds, New York, 1994 p. 459.
- [11] L. J. Lobree, A. W. Aylor, J. A. Reimer, A. T. Bell, *J. Catal.* 169 (1997) 188.
- [12] Y. Li, T. L. Slager, J. N. Armor, *J. Catal.* 150 (1994) 388.
- [13] G. R. Bamwenda, A. Ogata, A. Obuchi, J. Oi, K. Mizuno y J. Skrzypek, *Appl. Catal. B*, 6 (1995) 311.
- [14] D. K. Captain, M. Amiridis, *J. Catal.* 184 (1999) 377 ; and *J. Catal.* 194 (2000) 222.
- [15] D. K. Captain, C. Mihut, J. A. Dumesic, M. Amiridis, *Catal. Lett.* 83 (2002) 109.
- [16] K. Acke, M. Skoglundh, *Appl. Catal. B*, 20 (1999) 235.
- [17] F. Acke, B. Westerberg, M. Skoglundh, *J. Catal.* 179 (1998) 528.
- [18] C. Rottländer, R. Andorf, C. Plog, B. Krutzsh and M. Baerns, *Appl. Catal. B*, 11 (1996) 49.
- [19] V. Pitchon y A. Fritz, *J. Catal.* 186 (1999) 64.
- [20] M. Sasaki, H. Hamada, Y. Kintaichi, T. Ito, *Catal. Lett.* 15 (1992) 297.
- [21] B. J. Adelman, T. Beutel, G. D. Lei, W. M. H. Sachtler, *J. Catal.* 158 (1996) 327.
- [22] Y. Li, J. N. Armor, *J. Catal.* 150 (1994) 376.

- [23] F. Jayat, C. Lembarcher, U. Schubert, J. A. Martens, *Appl. Catal. B*, 21 (1999) 221.
- [24] P. Praserthdam, Ch. Chaisuk, A. Panit y K. Kraiwattanawong, *Appl. Catal. B*, 38 (2002) 227.
- [25] E. Joubert, X. Courtois, P. Marecot. C. Canaff, D. Duprez, *J. Catal* 243 (2006) 252.
- [26] F. Garin, P. Girard, S. Ringler, G. Maire, N. Davias, *App. Catal B, Env.* 20 (1999) 205.
- [27] S. Ringler, P. Girard, G. Maire, S. Hilaire, G. Roussy, F. Garin, *Appl. Catal. B* 20 (1999) 219.
- [28] F. Garin. *Catal. Today*, 89 (2004) 255.
- [29]. T. Inui, S. Iwamoto, S. Shimizu, *Proc. Ninth Int. Zeolite Conf.*, Vol. II, R. Von Balmoos, J.B. Higgins, M.M. T. Treacy (Eds) 1993 p.405.
- [30] R. Burch, J. A. Sullivan and T. C. Watling, *Catal. Today*, 42 (1998) 13.
- [31] R. Burch, P. J. Millington and A. P. Walker, *App. Catal. B*, 4 (1994) 65.
- [32] R. Burch, P. J. Millington, *Catal. Today*, 26 (1995) 185.
- [33] R. Burch and T. C. Watling, *Catal. Lett.* 37 (1996) 51.
- [34] B. K. Cho and J. E. Yie, *App. Catal. B*, 1 (1996) 263.
- [35] J.M. García-Cortés, J. Pérez-Ramírez, J.N 21. Rouzaud, A.R. Vaccaro, M.J. Illán-Gómez, C. Salinas-Martínez de Lecea, *J. Catal.* 8 (2003), 111.
- [36] R. Burch, J. A. Sullivan, *J. Catal.* 182 (1999) 489.
- [37] John Happel, *Isotopic Assessment of Heterogeneous Catalysis*, Academic Press, Inc. 1986, New York.
- [38] M. Xin, I. C. Hwang, D. H. Kim, S. I. Cho, S. I. Woo, *Appl. Catal. B*, 21 (1999) 183.
- [39] J.K. Brown, A.C. Lunzt, *Chem. Phys. Lett.* 204 (1993) 451.
- [40] A.T. Pasteur, X.C. Guo, T. Ali, M. Gruyters, D.A. King, *Surf. Sci.* 366 (1997) 564.
- [41] A. Kotsifa, D. I. Kondarides, X. E. Verykios, *Appl. Catal. B*, 72 (2007) 136.
- [42] R.A. Comelli, S.A. Canavese, C.A. Querini, N.S. Fígoli, *Appl. Catal. A*. 182 (1999) 275.
- [43] D. Duprez, M. Hajd-Aissa, J. Barbier, *Appl. Catal.* 49 (1989) 67.
- [44] J.Y. Jeon, H.Y. Kim and S.I. Woo, *Appl. Catal. B*, 44 (2003) 301.
- [45] J.Y. Jeon, H.Y. Kim and S.I. Woo, *Appl. Catal. B*, 44 (2003) 311.
- [46] A. Setiabudi, M. Makkee, J.A, Moulijn, *Appl. Catal. B*, 50 (2004) 185.
- [47] O. Gorce, F. Baudin, C, Thomas, P. da Costa, G. Djéga-Mariadassou, *Appl. Catal. B*, 54 (2004) 69.
- [48] S. C. Shen and S. Kawi. *Catalysis Today* 68 (2001) 245.
- [49] A. Bueno-López, M.J. Illán-Gómez, C. Salinas-Martínez, *Appl. Catal. A*. 302 (2006) 144

Figure captions

Figure 1. Scheme of the experimental device for the kinetic analysis. (a) Two-way valve, (b) three-way valve, (c) four-way electro-valve (switch), (d) mass flow controllers, (e) tubular quartz reactor, (f) horizontal furnace, (g) thermocoupler, (h) temperature controller, (i) filters (7 μ m), (j) high-sensitivity pressure transducers (0 – 0,6 mbar), (k) loop (50 μ l), (m) high precision regulation valve and (n) mass spectrometer.

Figure 2. Conversion of (■) NO_x and (□) C₃H₆ and NO₂ evolution (✕) on sample Pt-beta (r-0.5). Experimental conditions: 2262 ppm NO, 3400 ppm C₃H₆, 5 vol% O₂, balance He; P= 1 bar; GHSV = 50,000 h⁻¹ (experimental system described in ref. 35).

Figure 3. Switch C₃H₆/NO/O₂ → C₃H₆/Ar/O₂ over Pt-beta catalyst at 200°C. (◆) Ar, (◇) Ar⁻¹, (●) NO, (□) C₃H₆, (○) O₂, (■) CO₂.

Figure 4. Switch C₃H₆/Ar/O₂ → C₃H₆/NO/O₂ over Pt-beta catalyst at 200°C. (◆) Ar, (◇) Ar⁻¹, (●) NO, (□) C₃H₆, (○) O₂, (■) CO₂.

Figure 5. Switch C₃H₆/NO/O₂ → Ar/NO/O₂ over Pt-beta catalyst at 200°C. (◆) Ar, (◇) Ar⁻¹, (●) NO, (□) C₃H₆, (■) CO₂.

Figure 6. Switch Ar/NO/O₂ → C₃H₆/NO/O₂ over Pt-beta catalyst at 200°C. (◆) Ar, (◇) Ar⁻¹, (●) NO, (□) C₃H₆, (■) CO₂.

Figure 7. Switch C₃H₆/NO/O₂ → C₃H₆/NO/Ar over Pt-beta catalyst at 200°C. (◆) Ar, (◇) Ar⁻¹, (●) NO, (□) C₃H₆, (■) CO₂, (○) O₂.

Figure 8. Switch C₃H₆/NO/Ar → C₃H₆/NO/O₂ over Pt-beta catalyst at 200°C. (◆) Ar, (◇) Ar⁻¹, (●) NO, (□) C₃H₆, (■) CO₂, (○) O₂.

Figure 9. Temperature Programmed Desorption of sample Pt-beta after reaction at 200°C during 10 hours.

Figure 10. Switch C₃H₆/NO/O₂ → C₃H₆/Ar/O₂ over Pt-beta catalyst at 230°C. (◆) Ar, (◇) Ar⁻¹, (●) NO, (○) O₂, (■) CO₂.

Figure 11. Switch C₃H₆/Ar/O₂ → C₃H₆/NO₂/O₂ over Pt-beta catalyst at 230°C. (◆) Ar, (◇) Ar⁻¹, (Δ) NO₂, (■) CO₂.

Figure 12. (a) Switch Ar/NO/O₂ → C₃H₆/NO/O₂ over Pt-beta catalyst at 230°C (◆) Ar, (◇) Ar⁻¹, (●) NO, (○) O₂, (■) CO₂, (Δ) NO₂;

Figure 13. Temperature Programmed Desorption of sample Pt-beta after reaction at 230°C during 10 hours.

Figure 1

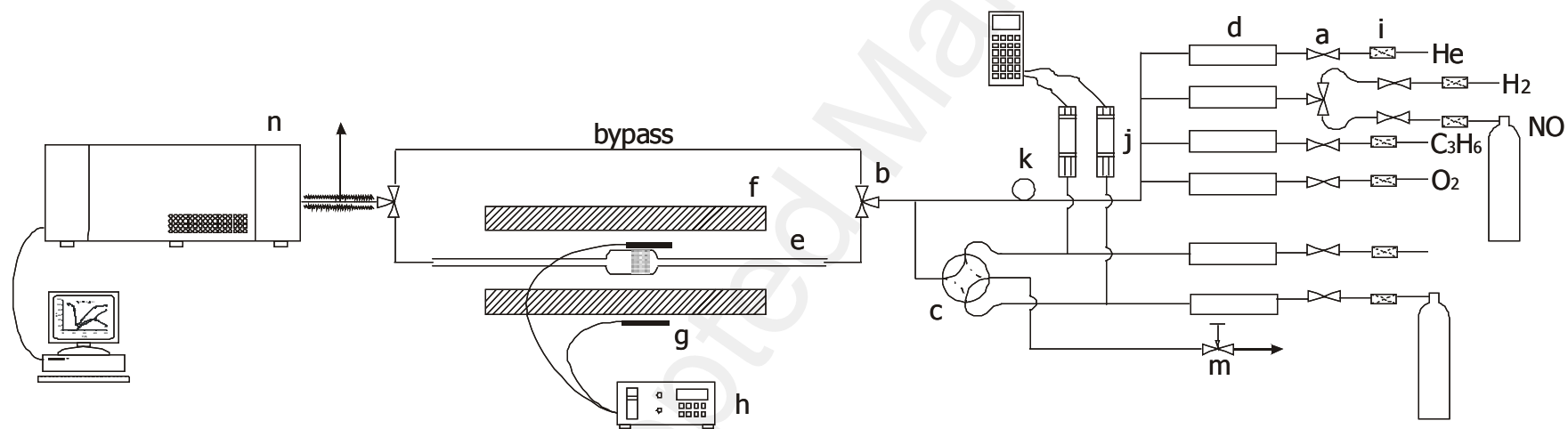


Figure 2

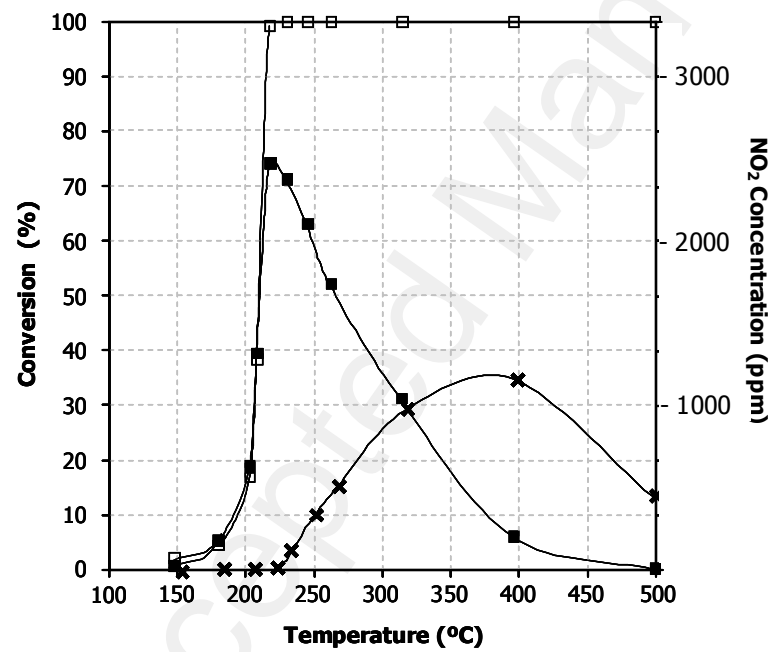
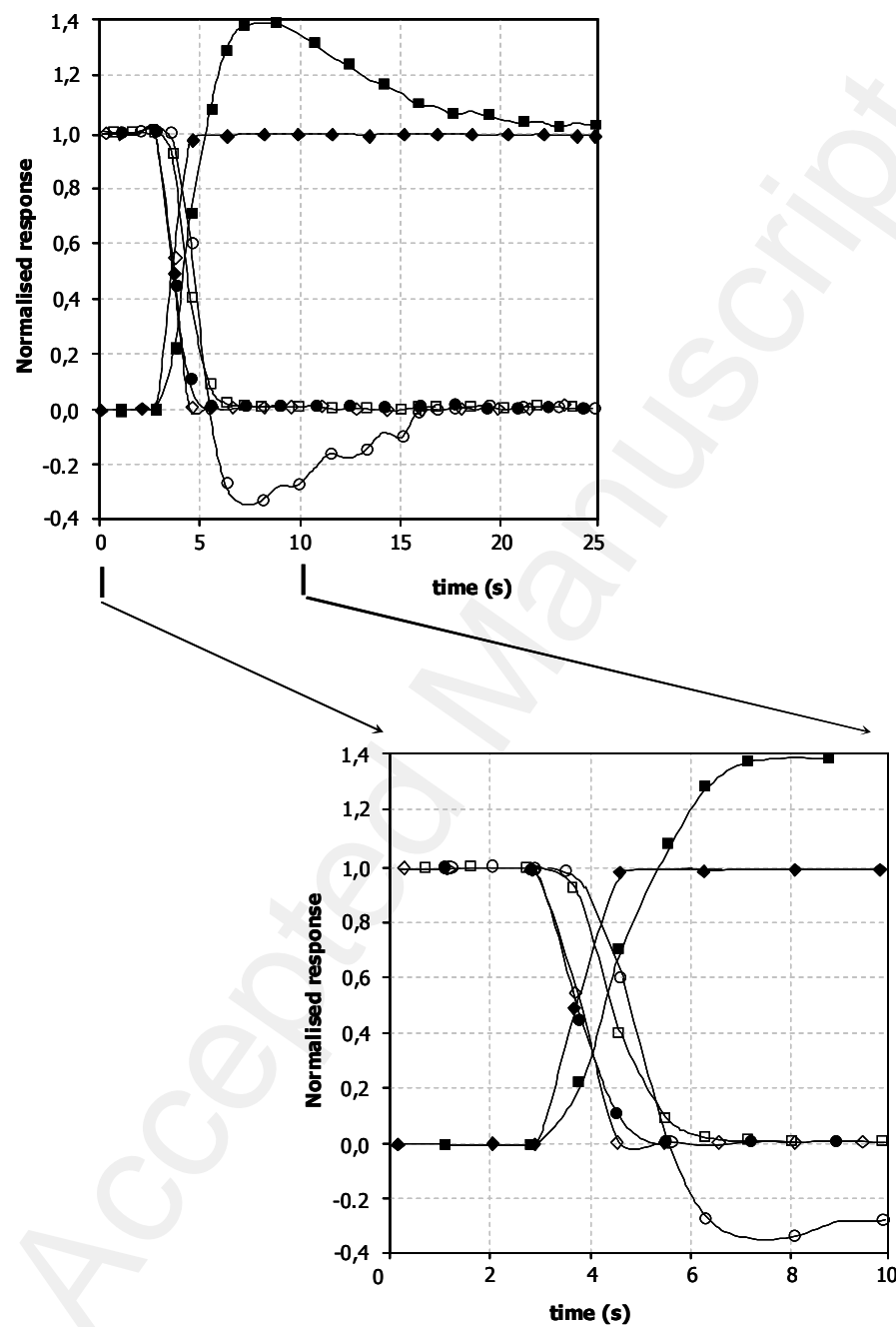


Figure 3



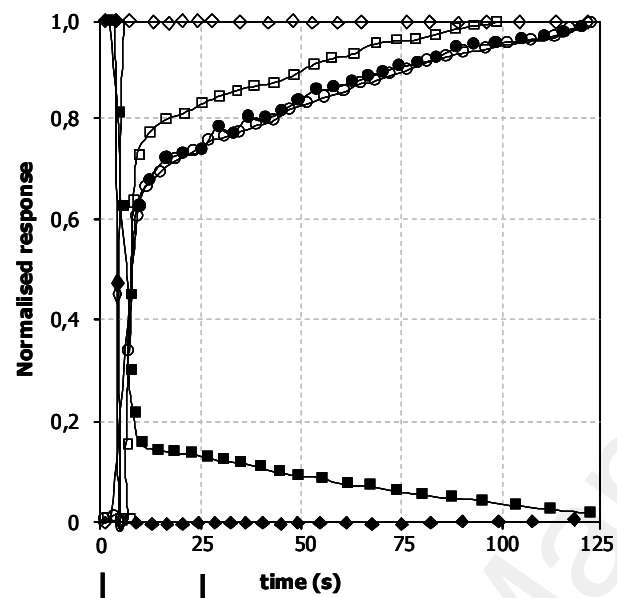


Figure 4

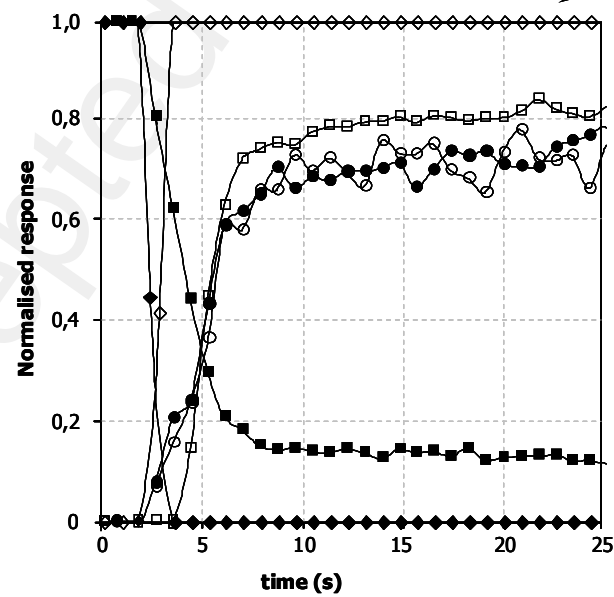


Figure 5

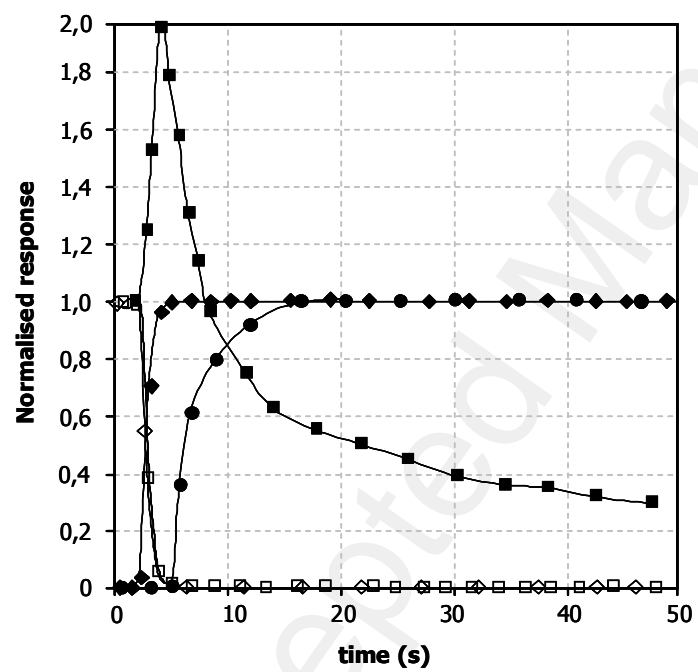


Figure 6

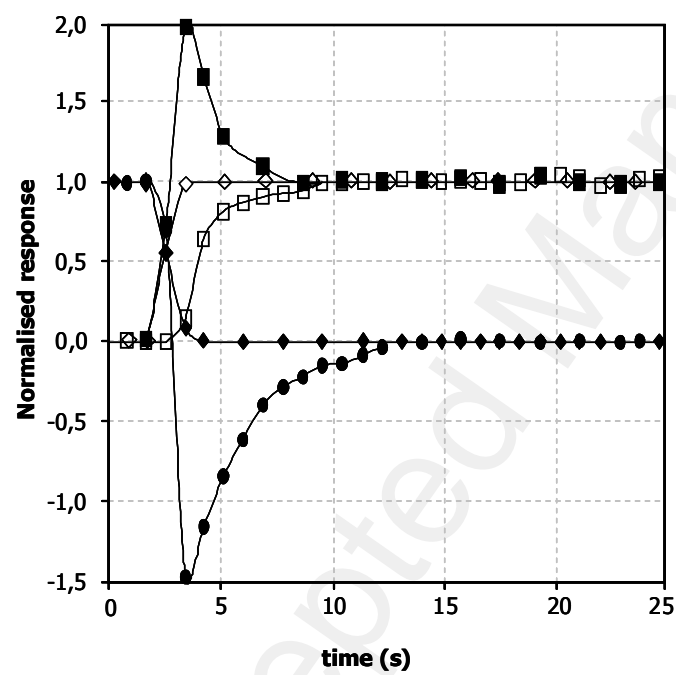


Figure 7

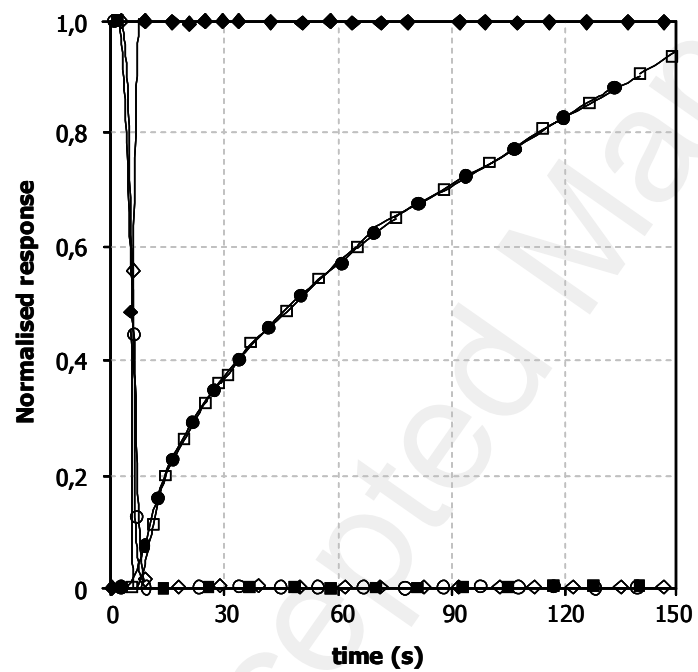


Figure 8

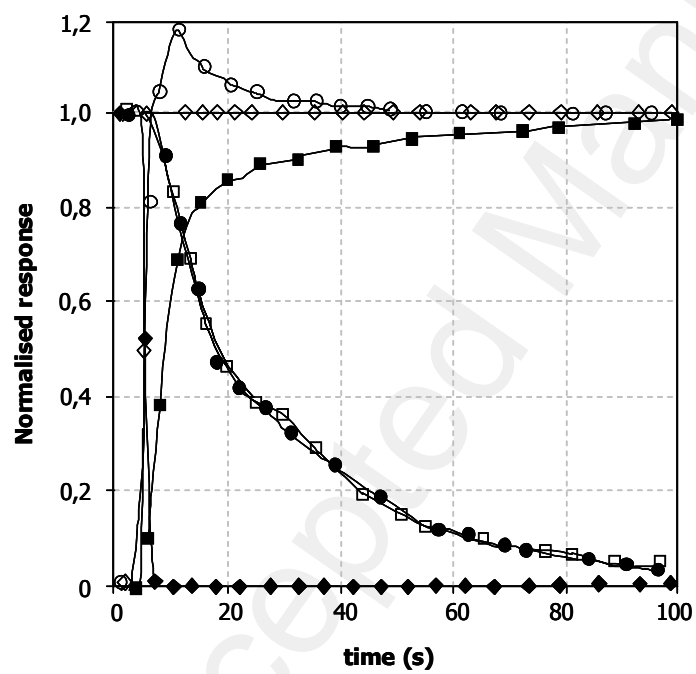


Figure 9

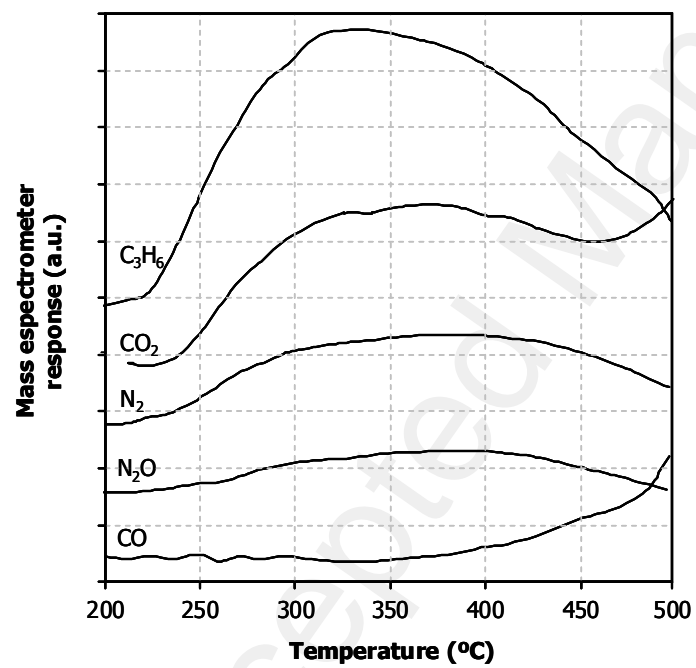


Figure 10

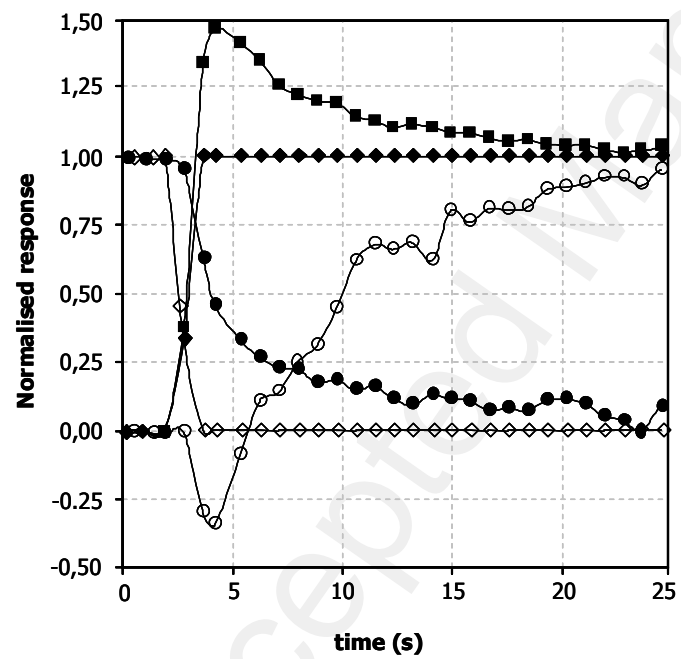
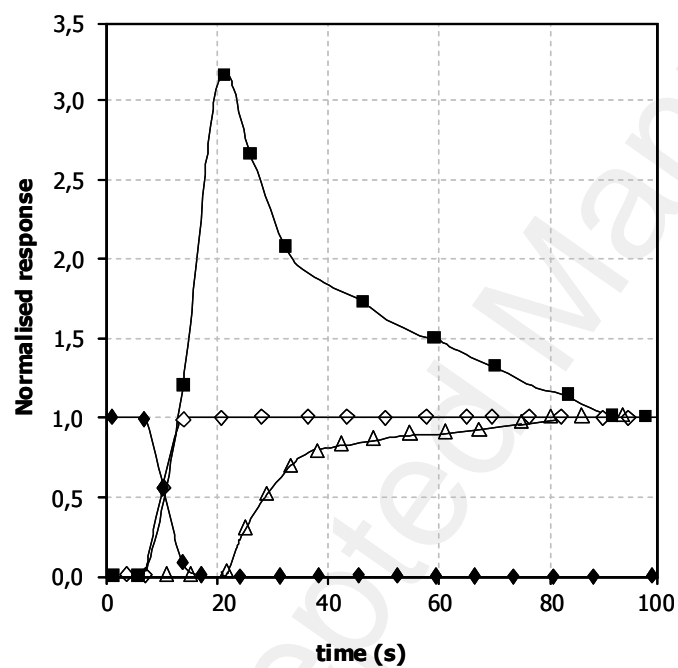


Figure 11



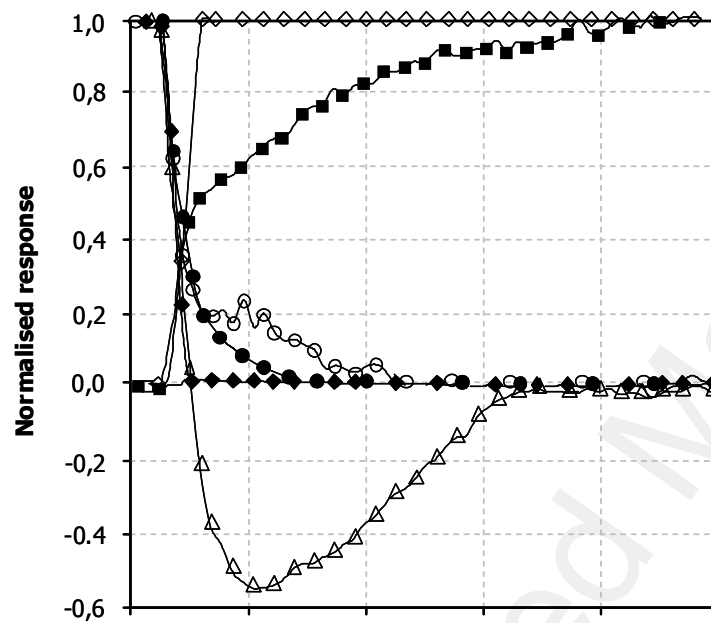


Figure 12

Figure 13

